



**HAL**  
open science

## The microwave spectrum of 2-methylthiazole: $^{14}\text{N}$ nuclear quadrupole coupling and methyl internal rotation

Thuy Nguyen, Vinh Van, Claudine Gutlé, Wolfgang Stahl, Martin Schwell,  
Isabelle Kleiner, Ha Vinh Lam Nguyen

► **To cite this version:**

Thuy Nguyen, Vinh Van, Claudine Gutlé, Wolfgang Stahl, Martin Schwell, et al.. The microwave spectrum of 2-methylthiazole:  $^{14}\text{N}$  nuclear quadrupole coupling and methyl internal rotation. The Journal of Chemical Physics, 2020, 152 (13), pp.134306. 10.1063/1.5142857 . hal-03182750

**HAL Id: hal-03182750**

**<https://hal.u-pec.fr/hal-03182750>**

Submitted on 26 Mar 2021


**HAL** is a multi-disciplinary open access archive for the deposit and dissemination of scientific research documents, whether they are published or not. The documents may come from teaching and research institutions in France or abroad, or from public or private research centers.

L'archive ouverte pluridisciplinaire **HAL**, est destinée au dépôt et à la diffusion de documents scientifiques de niveau recherche, publiés ou non, émanant des établissements d'enseignement et de recherche français ou étrangers, des laboratoires publics ou privés.

# The microwave spectrum of 2-methylthiazole: $^{14}\text{N}$ nuclear quadrupole coupling and methyl internal rotation

Cite as: J. Chem. Phys. **152**, 134306 (2020); <https://doi.org/10.1063/1.5142857>

Submitted: 17 December 2019 . Accepted: 10 March 2020 . Published Online: 02 April 2020

Thuy Nguyen, Vinh Van, Claudine Gutlé, Wolfgang Stahl , Martin Schwell, Isabelle Kleiner , and Ha Vinh Lam Nguyen 



View Online



Export Citation



CrossMark

## ARTICLES YOU MAY BE INTERESTED IN

[High-resolution infrared spectroscopy of jet cooled  \$\text{CH}\_2\text{Br}\$  radicals: The symmetric CH stretch manifold and absence of nuclear spin cooling](#)

The Journal of Chemical Physics **152**, 134305 (2020); <https://doi.org/10.1063/5.0002165>

[Low torsional barrier challenges in the microwave spectrum of 2,4-dimethylanisole](#)

The Journal of Chemical Physics **151**, 104310 (2019); <https://doi.org/10.1063/1.5116304>

[Local and global approaches to treat the torsional barriers of 4-methylacetophenone using microwave spectroscopy](#)

The Journal of Chemical Physics **152**, 074301 (2020); <https://doi.org/10.1063/1.5142401>

Lock-in Amplifiers  
up to 600 MHz



Watch



# The microwave spectrum of 2-methylthiazole: $^{14}\text{N}$ nuclear quadrupole coupling and methyl internal rotation

Cite as: J. Chem. Phys. 152, 134306 (2020); doi: 10.1063/1.5142857

Submitted: 17 December 2019 • Accepted: 10 March 2020 •

Published Online: 2 April 2020



Thuy Nguyen,<sup>1</sup> Vinh Van,<sup>2</sup> Claudine Gutlé,<sup>1</sup> Wolfgang Stahl,<sup>2</sup>  Martin Schwell,<sup>1</sup> Isabelle Kleiner,<sup>1</sup>   
and Ha Vinh Lam Nguyen<sup>1,a)</sup> 

## AFFILIATIONS

<sup>1</sup>Laboratoire Interuniversitaire des Systèmes Atmosphériques (LISA), CNRS UMR 7583, Université Paris-Est Créteil, Université de Paris, Institut Pierre Simon Laplace, 61 avenue du Général de Gaulle, F-94010 Créteil, France

<sup>2</sup>Institute of Physical Chemistry, RWTH Aachen University, Landoltweg 2, D-52074 Aachen, Germany

<sup>a)</sup> Author to whom correspondence should be addressed: lam.nguyen@lisa.u-pec.fr

## ABSTRACT

The rotational spectrum of 2-methylthiazole was recorded using two pulsed molecular jet Fourier transform microwave spectrometers operating in the frequency range of 2–40 GHz. Due to the internal rotation of the methyl group, all rotational transitions were split into A and E symmetry species lines, which were analyzed using the programs *XIAM* and *BELGI-C<sub>s</sub>-hyperfine*, yielding a methyl torsional barrier of 34.79675(18) cm<sup>-1</sup>. This value was compared with that found in other monomethyl substituted aromatic five-membered rings. The  $^{14}\text{N}$  quadrupole coupling constants were accurately determined to be  $\chi_{aa} = 0.5166(20)$  MHz,  $\chi_{bb} - \chi_{cc} = -5.2968(50)$  MHz, and  $\chi_{ab} = -2.297(10)$  MHz by fitting 531 hyperfine components. The experimental results were supplemented by quantum chemical calculations.

Published under license by AIP Publishing. <https://doi.org/10.1063/1.5142857>

## I. INTRODUCTION

The complexity of molecules studied by molecular jet Fourier transform microwave (MJ-FTMW) spectroscopy is steadily increasing, providing an enormous number of high resolution spectra for testing theoretical models. If the molecule can be described by using a semi-rigid rotor, a fit of high quality can be achieved using a rigid rotor Hamiltonian  $H_r$  supplemented by centrifugal distortion terms  $H_{cd}$ , taking into account even higher  $J$  and  $K$  transitions.

When a molecule contains a methyl group undergoing internal rotation hindered by a sufficiently low threefold potential barrier, its microwave spectrum exhibits splittings of all rotational lines into A and E torsional components and can no longer be treated using a semi-rigid rotor model. Several programs have been developed to treat the effect of internal rotation, i.e., a code written by Woods named after what was called the Internal Axis Method (IAM) at that time and we refer to as the Rho Axis Method (RAM) today,<sup>1</sup> *XIAM*,<sup>2</sup> *BELGI* in its  $C_s$  and  $C_1$  versions,<sup>3,4</sup> *Erham*,<sup>5</sup> and *RAM36*<sup>6</sup> (see <http://www.ifpan.edu.pl/~kisiel/prospe.htm>), where additional

terms to account for the internal rotation  $H_{ir}$  are added in the Hamiltonian. Some molecules associated with a high or intermediate barrier height can also be treated by the program *JB95* provided by Plusquellic,<sup>7</sup> as well as by the program *IAMCALC* that is integrated in Pickett's CALPGM suite of programs containing the *SPFIT* and *SPCAT* codes.<sup>8</sup> An overview of internal rotation programs can be found in Ref. 9.

A nucleus with a nuclear spin  $I \geq 1$  implies a spectroscopic electric nuclear quadrupole moment. Hyperfine structures occur in the microwave spectrum, i.e., the rotational levels with  $J > 0$  of the rigid rotor split into several hyperfine components. The size and pattern of the splittings depend on the respective transition. In the case of a  $^{14}\text{N}$  nucleus, the quadrupole moment is relatively small and can often be treated using a first order perturbation approximation.

The combination of a single  $^{14}\text{N}$  quadrupole coupling nucleus and methyl internal rotation can be handled with the program *RAM36*, which implies the molecular symmetry to be  $C_s$ .<sup>10</sup> With the program *XIAM*, the symmetry is not restricted to  $C_s$ .

However, *XIAM* often experiences difficulties in treating internal rotations with low barrier heights because (i) only a limited number of high order parameters can be fitted and (ii) the torsional interactions between different  $\nu_i$  states are not taken into account explicitly. The program *BELGI* has been extended in its hyperfine versions *BELGI-C<sub>s</sub>-hyperfine* and *BELGI-C<sub>1</sub>-hyperfine*, which can treat molecules with one internal rotor and one weakly coupling nucleus like <sup>14</sup>N. Its predictive power has been proven for several molecules containing one methyl rotor and a nitrogen nucleus such as *N-tert*-butylacetamide (C<sub>s</sub>),<sup>11</sup> *N*-ethylacetamide (C<sub>1</sub>),<sup>11</sup> 3-nitrotoluene (C<sub>s</sub>),<sup>12</sup> and 2-methylpyrrole (C<sub>s</sub>).<sup>13</sup>

Monomethyl derivatives of aromatic heterocyclic five-membered rings containing a nitrogen nucleus are ideally suited to test the Hamiltonian model because the  $V_3$  potential value of the methyl group covers a wide range from low barriers like those in 2-methylthiazole (34.9 cm<sup>-1</sup>)<sup>14</sup> and 4-methylisothiazole (105.8 cm<sup>-1</sup>)<sup>15</sup> to intermediate barriers such as in 4- and 5-methylthiazole (357.6 cm<sup>-1</sup> and 332.0 cm<sup>-1</sup>, respectively),<sup>16,17</sup> as well as in 2-, 4-, and 5-methyloxazole (252.0 cm<sup>-1</sup>, 428.3 cm<sup>-1</sup>, and 478.2 cm<sup>-1</sup>, respectively).<sup>18</sup> The first molecule mentioned above, 2-methylthiazole (2MTA), has been studied by Grabow *et al.* in the frequency range from 7 GHz to 13 GHz.<sup>14</sup> The  $V_3$  potential of 34.938(20) cm<sup>-1</sup> is the lowest of all examples. Two independent fits were performed in this previous investigation using the program *XIAM*.<sup>2</sup> In the first fit, 16 torsional transitions were fitted with a standard deviation of 443 kHz, which is more than 200 times the measurement accuracy. The centrifugal distortion constants could not be determined. In order to deduce the <sup>14</sup>N nuclear quadrupole coupling constants (NQCCs), only the splittings of 44 hyperfine components were fitted in a second fit with a standard deviation of 2.7 kHz. We believe that the Hamiltonian which describes the microwave spectrum of 2MTA requires some higher order terms, which are beyond the model used in *XIAM*. Therefore, we decided to (i) extend the dataset to cover a much larger frequency range from 2 GHz to 40 GHz to measure higher  $J$  and  $K$  values and (ii) refit the dataset using the program *BELGI-C<sub>s</sub>-hyperfine*<sup>11</sup> by including higher order terms in the Hamiltonian. The goal is to achieve a global fit with a standard deviation close to the measurement accuracy and a set of molecular parameters with high predictive power.

## II. EXPERIMENTAL AND QUANTUM CHEMICAL METHODS

### A. Quantum chemical calculations

#### 1. Structure optimizations

In order to predict the structure of 2MTA, the *Gaussian 03* program package<sup>19</sup> was used with three quantum chemistry methods: the Hartree–Fock self-consistent field method, the B3LYP density functional method, and the second-order Møller–Plesset perturbation theory with all electrons explicitly included (MP2ae). The Pople 6-311++G(d,p) basis set was chosen in all cases. These three levels of theory were chosen *a priori*, expected to provide reasonable predictions at an affordable cost for a medium-sized molecule like 2MTA. The equilibrium geometry of 2MTA optimized at the B3LYP/6-311++G(d,p) level is shown in Fig. 1. The rotational constants are collected in Table I.

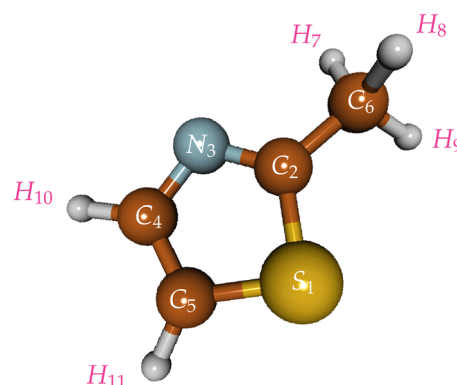


FIG. 1. Geometry of 2MTA optimized at the B3LYP/6-311++G(d,p) level of theory.

Four conformations are of interest for studying the rotation of the methyl group relative to the thiazole ring, which can be characterized by the value of the dihedral angle  $\alpha = \angle(S_1, C_2, C_6, H_9)$ . In the first conformation at  $\alpha = 0^\circ$ , the proton  $H_9$  is eclipsed with the sulfur atom if we look along the  $C_2$ – $C_6$  bond. The second one with  $\alpha = 60^\circ$  has the  $H_8$  atom eclipsed with the nitrogen atom. In

TABLE I. The rotational constants (in MHz) of the most stable geometry of 2-methylthiazole calculated at the B3LYP/6-311++G(d,p), HF/6-311++G(d,p), and MP2(ae)/6-311++G(d,p) levels of theory. The dihedral angle  $\alpha$  is defined as  $\angle(S_1, C_2, C_6, H_9)$ . For comparison, the data for the conformation with  $\alpha = 60^\circ$  calculated at the MP2(ae)/6-311++G(d,p) level of theory are also given.

	(e) <sup>a</sup>	(00) <sup>b</sup>	(0) <sup>c</sup>
B3LYP/6-311++G(d,p) $\alpha = 60^\circ$			
A	5287.361	5256.606	5256.607
B	3238.812	3219.713	3219.711
C	2033.933	2021.676	2021.677
HF/6-311++G(d,p) $\alpha = 60^\circ$			
A	5414.526	5388.873	5388.873
B	3273.155	3254.854	3254.854
C	2065.917	2054.512	2054.512
MP2(ae)/6-311++G(d,p) $\alpha = 32.9^\circ$			
A	5319.383	5287.236	5287.236
B	3273.476	3250.856	3250.856
C	2052.720	2038.443	2038.443
MP2(ae)/6-311++G(d,p) $\alpha = 60^\circ$			
A	5317.821	5284.436	5284.436
B	3271.103	3249.920	3249.920
C	2051.308	2037.267	2037.267

<sup>a</sup>Equilibrium constants.

<sup>b</sup>Constants including the vibrational correction.

<sup>c</sup>Constants including the vibrational correction and the centrifugal distortion.

**TABLE II.** Dihedral angle  $\alpha$ , the difference  $\Delta\alpha$  between the conformers, the energy at the stationary points  $E$ , the energy difference  $\Delta E$  between the conformers, the energy with vibrational corrections  $E+ZPE$ , and the energy difference  $\Delta(E+ZPE)$  between the conformers of 2-methylthiazole obtained while rotating the methyl group.

Method	$\alpha/^\circ$	$\Delta\alpha/^\circ$	Type	$E/\text{Hartree}$	$\Delta E/\text{cm}^{-1}$	$E+ZPE/\text{Hartree}$	$\Delta(E+ZPE)/\text{cm}^{-1}$
B3LYP	0.0		Max	-608.453 587 36		-608.371 336 836	
	60.0	60.0 $\rightarrow$ 0.0	Min	-608.453 382 733	52.61	-608.371 356 133	42.29
HF	0.0		Max	-606.405 361 535		-606.317 339 835	
	60.0	60.0 $\rightarrow$ 0.0	Min	-606.406 317 233	122.20	-606.317 383 933	96.74
MP2	0.0	0.0 $\rightarrow$ 32.9	Max	-607.496 377 132	-29.37	-607.413 384 132	6.41
	32.9	60.0 $\rightarrow$ 32.9	Min	-607.496 390 530	-25.52	-607.413 381 230	22.98
	60.0	60.0 $\rightarrow$ 0.0	Max	-607.496 307 838 7	-3.84	-607.413 391 637	16.57

the third conformation at  $\alpha \approx 30^\circ$ , the  $C_6-H_7$  bond is roughly perpendicular to the ring plane. Finally, the fourth conformation at  $\alpha \approx 90^\circ$  with the  $C_6-H_9$  bond being roughly perpendicular to the ring plane is equivalent to the  $\alpha \approx 30^\circ$  position, assuming that the ring is planar as expected for an aromatic system. Due to symmetry, each of these four conformations appears three times during a full rotation of the methyl group about the  $C_2-C_6$  bond. As summarized in Table II, they all give rise to a stationary point of the electrostatic energy at the MP2(ae)/6-311++G(d,p) level with those at  $\alpha = 32.9^\circ$  and  $\alpha = 87.1^\circ$  as the most stable rotamers and two saddle points at  $\alpha = 0^\circ$  and  $60^\circ$ , while only the first two conformations are found to be stationary in calculations at the B3LYP/6-311++G(d,p) and HF/6-311++G(d,p) levels with the most stable rotamer at  $\alpha = 60^\circ$ .

For all the above-mentioned conformers, the zero point energy (ZPE) correction to the electrostatic energy was calculated as given in Table II. For all maxima, geometry optimizations to a first-order transition state were performed in addition by using the Berny algorithm,<sup>20</sup> which yielded the same results as those given in Table II. With the MP2 method, the difference of the ZPE corrections for the double-minimum and barrier dividing it is larger than the value for this barrier, indicating that the zero-point vibrational level lies above the barrier at  $\alpha = 60^\circ$ . However, the difference of the ZPE corrections for the minima and the maxima of the potential surface is smaller than the value of the three-fold barrier, suggesting that the  $V_6$  contribution to the potential is of minor importance and therefore, the potential can be effectively described by a  $V_3$  term. The Cartesian coordinates of the atoms are reported in Table S-I of the supplementary material.

## 2. Methyl internal rotations

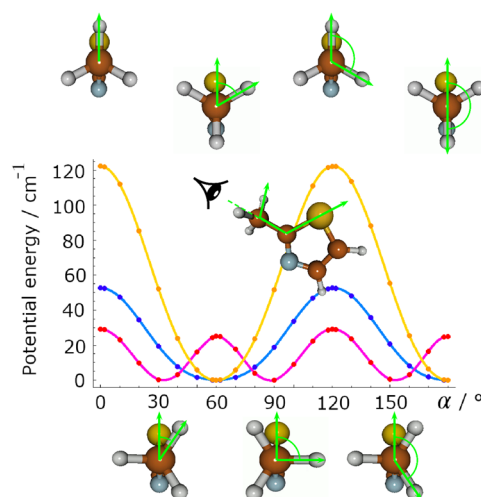
Potential energy scans were generated by rotating the methyl group about the  $C_2-C_6$  bond. The dihedral angle  $\alpha$  was varied in a grid of  $10^\circ$  ( $2^\circ$  around the stationary points). All other geometry parameters were optimized. The potential energy curves showing the rotation of the methyl group are presented in Fig. 2, where the minima of all curves have been translated to the energy origin. The corresponding data points are available in Table S-II of the supplementary material. While the potential curves calculated with the B3LYP and HF methods show normal threefold potentials without  $V_6$  contribution, the MP2 method predicts  $V_6$  as the dominating term with a value of  $26.92 \text{ cm}^{-1}$  and a  $V_3$  contribution of  $6.92 \text{ cm}^{-1}$ . These values were obtained by parameterizing the data points given

in Table S-II with a one-dimensional Fourier expansion as

$$V(\alpha) = -607.496\,842 \text{ Hartree} + \frac{6.92 \text{ cm}^{-1}}{2} \cos(3\alpha) + \frac{26.92 \text{ cm}^{-1}}{2} \cos(6\alpha) - \frac{2.82 \text{ cm}^{-1}}{2} \cos(9\alpha).$$

Therefore, they slightly deviate from those given in Table II.

Our best estimate for the  $V_3$  potential includes the ZPE correction, as shown in Table II under  $\Delta(E+ZPE)$ , whose value depends on the method in use. The Hartree-Fock method is not expected to be quantitative, whereas the  $V_3$  potential of  $42.29 \text{ cm}^{-1}$  from calculations using the density functional is presumed to be more quantitatively realistic. Finally, as the MP2 results are not in agreement with those of the Hartree-Fock ( $96.74 \text{ cm}^{-1}$ ) and the B3LYP methods, the experimental results are important to validate the results from calculations. We emphasize that the small value of the methyl

**FIG. 2.** Potential energy curves of 2-methylthiazole (in  $\text{cm}^{-1}$ ) obtained by rotating the methyl group about the  $C_2-C_6$  bond. The dihedral angle  $\alpha = \angle(S_1, C_2, C_6, H_9)$  was varied in a grid of  $10^\circ$  ( $2^\circ$  around stationary points), while all other molecular parameters were optimized at the B3LYP/6-311++G(d,p) (in blue), HF/6-311++G(d,p) (in orange), and MP2(ae)/6-311++G(d,p) (in magenta) levels of theory. The energies are relative to the energetically lowest conformations.

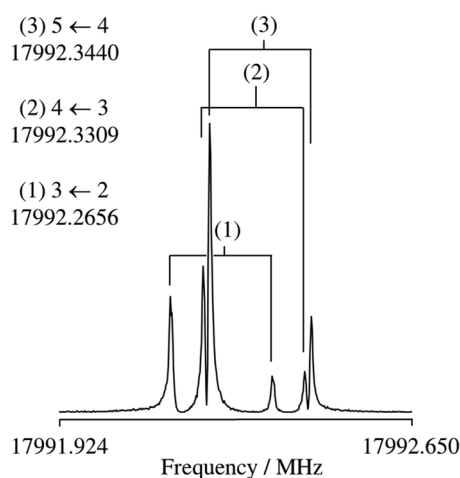


**FIG. 3.** The  $4_{04} \leftarrow 3_{13}$  transition of the A species of 2MTA with its quadrupole hyperfine components given as  $F' \leftarrow F$ . The splittings indicated by brackets are due to the Doppler effect. For this spectrum, 41 free-induction decays were co-added.

torsional barrier of 2MTA is a significant challenge for quantum chemistry.

## B. Measurements

2MTA, purchased from TCI Europe, Zwijndrecht, Belgium, has a stated purity of 98% and was used without further purification. The colorless liquid with a typical aromatic smell was placed on a pipe cleaner in a stainless steel tube upstream the nozzle. Under a helium stream at a backing pressure of 2 bars, the helium-2MTA mixture was expanded into the vacuum chamber. The spectra were recorded using two MJ-FTMW spectrometers operating in the frequency ranges from 2 GHz to 26.5 GHz (the Aachen big cavity)<sup>21</sup> and 26.5–40 GHz (the Paris small cavity).<sup>22</sup> All lines appear as doublets because of the Doppler effect. A typical spectrum is shown in Fig. 3. Some intense lines can be measured with a full width at half height smaller than 20 kHz, corresponding to a measurement accuracy of 2 kHz, but in most cases, the linewidths are larger. In some transitions, small splittings up to 10 kHz were observed, probably due to proton spin–spin and spin–rotation coupling. The measurement accuracy is thus about 3 kHz. In all fits carried out in the present work, all lines were equally weighted.

## III. MICROWAVE SPECTRUM

### A. $^{14}\text{N}$ nuclear quadrupole coupling

In the first step, we neglected the methyl internal rotation effect and treated 2MTA as an effective rigid rotor with  $^{14}\text{N}$  nuclear quadrupole coupling. The 34 A species transitions (including their hyperfine splittings) reported in Ref. 14 were refitted with the program XIAM in its rigid rotor mode with a root-mean-square (rms) deviation of about 3 kHz. This fit allowed us to predict the whole rigid rotor spectrum with sufficient accuracy to measure new A

species lines in the frequency range from 2 GHz to 40 GHz. All lines appear as multiplets with a different number of components, which could be straightforwardly attributed to the  $^{14}\text{N}$  hyperfine structure. Three rotational constants  $A$ ,  $B$ , and  $C$ , five quartic centrifugal distortion constants, and two NQCCs were fitted for a total of 278 A species hyperfine components to measurement accuracy. The molecular parameters are summarized as Fit XIAM A in Table III.

### B. Methyl internal rotation

In the second step, we took into account the methyl internal rotation by including the 26 E species transitions from Ref. 14 in the fit, and achieved a standard deviation of over 400 kHz. With the parameters from this fit, a prediction of the E species frequencies was performed between 2 GHz and 40 GHz. However, the predicted frequencies did not match the experimental ones. Consequently, the assignments of the hyperfine structure were carried out by analyzing the hyperfine splittings instead of the absolute frequencies. Finally, 278 A species and 253 E species lines were measured and fitted using the program XIAM with an rms deviation of 455.9 kHz, similar to the result of Ref. 14. The molecular parameters from the so-called Fit XIAM A/E are presented in Table III. A list of all fitted transitions is given in Table S-III of the supplementary material. All attempts to reduce the large rms deviation using XIAM failed.

In order to achieve a global fit with measurement accuracy, the program *BELGI- $C_s$ -hyperfine*<sup>11</sup> was applied. By floating 21 parameters (plus the reduced rotational constant  $F$  of the methyl group fixed at the value from the XIAM A/E fit), which are the NQCCs  $\chi_{aa}$ ,  $\chi_{bb}$ , and  $\chi_{ab}$ , together with the three rotational constants  $A$ ,  $B$ ,  $C$ , five centrifugal distortion constants  $\Delta_J$ ,  $\Delta_{JK}$ ,  $\Delta_K$ ,  $\delta_J$ , and  $\delta_K$ , the  $D_{ab}$  parameter multiplying the off-diagonal  $\{P_a, P_b\}$  term, the torsional potential barrier height  $V_3$ , the unitless parameter  $\rho$ , which together with  $F$ , is associated with  $P_a P_a$ , and seven additional terms beyond the rigid top–rigid frame model, the rms deviation of the fit decreases to 3.2 kHz. All out-of-plane terms were set to zero due to the  $C_s$  symmetry of 2MTA. The *BELGI- $C_s$ -hyperfine* parameters in the rho axis system are given in Table IV, and the parameters that could be transferred to the principal axis system are presented in Table III.

## IV. DISCUSSION

The *BELGI- $C_s$ -hyperfine* code improves the rms deviation of 2MTA to measurement accuracy by adding 7 effective parameters, which are not available in the XIAM code. The operators containing the  $(1 - \cos 3\alpha)$  term led to the most significant changes of the fit. The rotational constants  $A$ ,  $B$ , and  $C$  obtained from both fits, the XIAM A/E and the *BELGI* fits, are well-determined and they agree within 0.4%. Better agreement is not expected because (i) different approaches are used in the two codes, (ii) different sets of parameters are used, and (iii) the conversion of RAM parameters to PAM parameters is not unique. The accuracy of the rotational constants is higher by two orders of magnitude in the XIAM A fit. The rms deviation of 3.0 kHz of the XIAM A fit, which is essentially the measurement accuracy, indicates that for the A species of 2MTA, a semi-rigid rotor model with centrifugal distortion corrections is

**TABLE III.** Molecular parameters in the principal axis system obtained using the *XIAM* code (*XIAM A* and *XIAM A/E*) and the *BELGI-C<sub>s</sub>-hyperfine* code (*BELGI*). For the *BELGI* fit, the molecular parameters in the rho axis system were transformed into the principal axis system. Details on the conversion are given in Ref. 23.

Par. <sup>a</sup>	Unit	<i>XIAM A</i>	<i>XIAM A/E</i>	<i>BELGI</i> hyperfine	MP2(ae) <sup>b</sup>
<i>A</i>	MHz	5490.326 86(14)	5343.110(23)	5323.498(49)	5284.436
<i>B</i>	MHz	3266.223 383(76)	3266.069 7(98)	3264.195 5(93)	3249.920
<i>C</i>	MHz	2052.328 264(68)	2052.396 3(88)	2051.508 0(15)	2037.267
$\Delta_J$	kHz	0.240 07(63)	0.458(72)	0.237 63(54)	0.223 817
$\Delta_{JK}$	kHz	1.281 7(26)	1.01(29)		0.257 817
$\Delta_K$	kHz	15.369 7(56)			0.883 085
$\delta_J$	kHz	0.078 88(27)	0.180(30)		0.073 732
$\delta_K$	kHz	0.740 4(20)	1.00(22)		0.369 655
<i>F</i> <sub>0</sub>	GHz		159 <sup>c</sup>		159
<i>F</i>	GHz		164.515 5 <sup>d</sup>	164.515 5 <sup>e</sup>	
$\rho$			0.033 540 793 <sup>d</sup>	0.033 106 70(95)	
<i>V</i> <sub>3</sub>	cm <sup>-1</sup>		34.796 75(18)	34.253 5(12)	6.92 <sup>f</sup>
<i>D</i> <sub>pi2J</sub>	kHz		-88.7(24)		
<i>D</i> <sub>pi2K</sub>	MHz		0.331 0(79)		
$\angle(i,a)$	°		4.458 9(15)	4.641 3(31)	5.581 7
$\angle(i,b)$	°		94.458 9(15)	94.641 3(31)	95.581 1
$\angle(i,c)$	°		90.0 <sup>g</sup>	90.0 <sup>g</sup>	89.920 4
$\chi_{aa}$	MHz	0.540 7(16)	0.44(17)	0.516 6(20)	0.462 <sup>h</sup>
$\chi_{bb} - \chi_{cc}$	MHz	-5.315 9(24)	-5.21(27)	-5.296 8(50)	-5.044 <sup>h</sup>
$\chi_{ab}$ <sup>i</sup>	MHz			-2.297(10)	-2.464 <sup>h</sup>
<i>N</i> <sub>A</sub> / <i>N</i> <sub>E</sub> <sup>j</sup>		278/0	278/253	278/253	
<i>rms</i> <sup>k</sup>	kHz	3.0	455.9	3.2	

<sup>a</sup>Standard error in parentheses in the unit of the last digits. Watson's *A* reduction and *I'* representation were used.<sup>b</sup>Values calculated at the MP2(ae)/6-311++G(d,p) level, including the vibrational and centrifugal distortion corrections with  $\alpha = 60^\circ$ , except the values for the NQCCs.<sup>c</sup>Fixed to the *ab initio* value.<sup>d</sup>Derived parameter.<sup>e</sup>Not fitted. Fixed to the *XIAM A/E* value.<sup>f</sup>The potential energy contains a leading *V*<sub>6</sub> contribution of 26.92 cm<sup>-1</sup>.<sup>g</sup>Fixed due to symmetry.<sup>h</sup>Calculated at the B3PW91/6-311+G(d,p)//MP2(ae)/6-311++G(d,p) level of theory. Values from Ref. 14 are  $\chi_{aa} = 0.5239(30)$  MHz,  $\chi_{bb} - \chi_{cc} = -5.239(15)$  MHz, and  $\chi_{ab} = -2.279(14)$  MHz.<sup>i</sup>Cannot be fitted in Fit *XIAM A* and not determinable in Fit *XIAM A/E*.<sup>j</sup>Number of fitted A and E species lines.<sup>k</sup>Root-mean-square deviation of the fit.

satisfactory. The inertial defect  $\Delta_c = I_c - I_a - I_b = -3.083 \text{ u}\text{\AA}^2$  confirms that the heavy atom skeleton is planar with a pair of methyl hydrogen atoms out of plane. This value is very close to that found for the isomers 4-methylthiazole ( $-3.092 \text{ u}\text{\AA}^2$ )<sup>16</sup> and 5-methylthiazole ( $-3.077 \text{ u}\text{\AA}^2$ ).<sup>17</sup>

The rotational constants obtained from the *XIAM A* fit agree with the constants calculated at the MP2(ae)/6-311++G(d,p) level of theory, including the vibrational correction and the centrifugal distortion. The deviation is 1.10% for *A*, 0.50% for *B*, and 0.74% for *C* with respect to the *XIAM* values. They are even smaller if the values obtained for the equilibrium structure are taken (0.48% for *A*, -0.16% for *B*, and 0.06% for *C*), suggesting that geometry parameters of the equilibrium structure calculated at the MP2(ae)/6-311++G(d,p) level of theory could be used directly to support the

vibrational ground state assignment in methyl substituted thiazoles. The results from calculations using the more cost-efficient B3LYP method are less accurate, but also reasonable.

The calculated centrifugal distortion constants are quite different from those deduced in Fit *XIAM A*, but in the same order of magnitude as the values in Fit *XIAM A/E*. The large rms deviation in the latter fit leads to low accuracy of the experimental values. The well-determined constants from the *BELGI-C<sub>s</sub>-hyperfine* fit refer to the rho axis system and cannot be directly compared with the calculated values, which refer to the principal axis system.

The NQCCs cannot be determined well in the *XIAM A/E* fit because of the large rms deviation, but in the *XIAM A* and the *BELGI* fits, they are accurately deduced and agree nicely in both

**TABLE IV.** Molecular parameters of 2MTA in the rho axis system obtained using the *BELGI-C<sub>s</sub>-hyperfine* code.

Par. <sup>a</sup>	Unit	Value	Operator
A	MHz	5318.408(48)	$P_a^2$
B	MHz	3269.285 7(64)	$P_b^2$
C	MHz	2051.508 1(15)	$P_c^2$
$D_{ab}$	MHz	102.256(68)	$\{P_a, P_b\}$
$\Delta_J$	kHz	0.237 63(54)	$-P^4$
$\Delta_{JK}$	kHz	0.976 8(28)	$-P^2 P_a^2$
$\Delta_K$	kHz	-2.978(14)	$-P_a^4$
$\delta_J$	kHz	0.077 42(24)	$-2P^2(P_b^2 - P_c^2)$
$\delta_K$	kHz	0.751 7(27)	$-\{P_a^2, (P_b^2 - P_c^2)\}$
$2\chi_{aa}$	MHz	1.472 5(34)	
$2\chi_{bb}$	MHz	-6.252 8(31)	
$2\chi_{ab}$	MHz	-4.232(21)	
$V_3$	cm <sup>-1</sup>	34.253 5(12)	$(1/2)(1 - \cos 3\alpha)$
$\rho$	Unitless	0.033 106 70(95)	$P_a P_\alpha$
F	cm <sup>-1</sup>	5.487 65 <sup>b</sup>	$P_a^2$
$\Delta_{ab}$	MHz	-1.110(23)	$P_a^2 \{P_a, P_b\}$
$F_v$	MHz	1.623 4(67)	$(1 - \cos 3\alpha)P^2$
$k_5$	MHz	31.971(78)	$(1 - \cos 3\alpha)P_a^2$
$c_2$	MHz	0.466 6(53)	$(1 - \cos 3\alpha)(P_b^2 - P_c^2)$
$d_{ab}$	MHz	-3.192(61)	$(1 - \cos 3\alpha)\{P_a, P_b\}$
$k_1$	MHz	-0.102 74(62)	$P_a^3 P_\alpha$
$c_4$	kHz	4.82(21)	$P_a P_\alpha, (P_b^2 - P_c^2)$
$N_A/N_E/N_q^c$		93/83/531	
$rms^d$	kHz	3.2	

<sup>a</sup>All parameters refer to the rho axis system and cannot be directly compared to those referred to the principal axis system.  $P_a$ ,  $P_b$ , and  $P_c$  are the components of the overall rotation angular momentum,  $P_\alpha$  is the angular momentum of the internal rotor rotating about the internal rotor axis by an angle  $\alpha$ .  $\{u, v\}$  is the anti-commutator  $uv + vu$ . The product of the parameter and operator from a given row yields the term actually used in the vibration-rotation-torsion Hamiltonian, except for  $F$ ,  $\rho$ , and  $A$ , which occur in the Hamiltonian in the form  $F(P_\alpha - \rho P_a)^2 + AP_a^2$ , where  $F = h/8\pi^2 c r I_\alpha$  (cm<sup>-1</sup>). Statistical uncertainties are shown as one standard uncertainty in the last digit.

<sup>b</sup>Fixed to the value from the *XIAM* A/E fit.

<sup>c</sup>Number of A and E species transitions as well as hyperfine components.

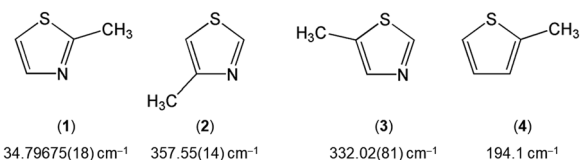
<sup>d</sup>Root-mean-square deviation of the fit.

fits as well as with the values from Ref. 14. Due to the rather low barrier to internal rotation of the methyl group, the expectation value of the operator  $\{P_a, P_b\}$  is not negligible and therefore,  $\chi_{ab}$  could be determined experimentally. Calculations of the <sup>14</sup>N NQCCs were performed by Bailey at the B3PW91/6-31G(2d,2pd) level based on optimized molecular structures as given in Ref. 24. Using the density functional B3PW91, Bailey also reported two possible orientations of the methyl group where the in-plane C<sub>6</sub>-H<sub>9</sub> bond is in the *cis* or *trans* position with respect to the nitrogen atom. This agrees well with our results obtained with the B3LYP and HF methods, and the *cis* and *trans* conformers in Ref. 24 correspond to our conformers at  $\alpha = 0^\circ$  and  $\alpha = 60^\circ$ , respectively. The calculated NQCCs for the *cis* conformer are  $\chi_{aa} = 0.449$  MHz,  $\chi_{bb} - \chi_{cc} = -5.269$  MHz, and  $|\chi_{ab}| = 2.338$  MHz. The respective values for the *trans* rotamer are 0.517 MHz, -5.186 MHz, and

2.307 MHz, showing that the experimentally deduced  $\chi_{aa}$  value is much closer to the predicted value of the *trans* conformation with  $\alpha = 60^\circ$ .

The program *XIAM* yielded a methyl torsional barrier of 34.79675(18) cm<sup>-1</sup>, which is very close to the value of 34.2535(12) cm<sup>-1</sup> determined by *BELGI-C<sub>s</sub>-hyperfine*. The calculated barrier heights  $\Delta E$  given in Table II are 52.61 cm<sup>-1</sup>, 122.20 cm<sup>-1</sup>, and 29.37 cm<sup>-1</sup> using the B3LYP, HF, and MP2 methods, respectively. While the values predicted with the HF method are far from being accurate, the B3LYP method overestimates and the MP2 method underestimates the torsional barrier height. Considering the ZPE corrections have shifted the predicted barriers to the right direction for the B3LYP and HF methods with the respective values of 42.29 cm<sup>-1</sup> and 96.74 cm<sup>-1</sup>, but the results still do not satisfy the experimental requirements. For the MP2 method, it is difficult to evaluate because the ZPE corrected difference is greater than the non-corrected difference. Many of our previous studies have pointed out the challenge of predicting the torsional barrier heights.<sup>25</sup> The calculated values vary strongly depending on the level of theory in use.<sup>26-28</sup> No method currently exists to solve this problem in general. If the  $V_3$  and  $V_6$  terms are fitted using the program *XIAM*, both of them could be determined with respective values of 31.88(21) cm<sup>-1</sup> and 17.2(12) cm<sup>-1</sup>, but the correlation between them is -1.000 because only rotational transitions from the vibrational ground state are available in the dataset. If the  $V_6$  term is fixed in the *XIAM* A/E fit or in the *BELGI* fit to different values from 0 to 20 cm<sup>-1</sup>, the fits converge and the rms deviations remain almost unchanged. The  $V_3$  value changes according to the fixed value of  $V_6$  due to correlation. We conclude that the quantity of  $V_6$  contribution cannot be determined and further investigation, including higher torsional state is needed to lift its correlation with  $V_3$ . Therefore, the leading  $V_6$  contribution found in calculations at the MP2/6-311++G(d,p) level cannot be validated by the experiment.

The  $V_3$  potential of 2MTA (1) decreases approximately by one order of magnitude compared to the barrier heights of 357.55(14) cm<sup>-1</sup> and 332.02(81) cm<sup>-1</sup> observed for 4- (2)<sup>16</sup> and 5-methylthiazole (3),<sup>17</sup> respectively (for molecule numbering, see Fig. 4). If we consider that the electronic environment around the sulfur atom and the nitrogen atom were similar, there would be a methyl group with C<sub>3v</sub> symmetry attached to a C<sub>2v</sub> frame. In such cases, the  $V_3$  contribution of the potential would be zero and only a  $V_6$  term would exist in the potential function expression. However, in 2MTA (1), the frame symmetry is not C<sub>2v</sub>. Therefore, the electronic distribution is out of balance, which causes a low, but significant  $V_3$  potential term. If the nitrogen atom disappears from the ring, as in the case of 2-methylthiophene (4), the barrier height

**FIG. 4.** Comparison of the methyl torsional barriers of 2MTA (1) (this work) and its two isomers 4- (2)<sup>16</sup> and 5-methylthiazole (3)<sup>17</sup> as well as 2-methylthiophene (4).<sup>29</sup>



increases to  $194.1\text{ cm}^{-1}$ ,<sup>29</sup> indicating that not only the position of the methyl group, but also the presence of the nitrogen atom is crucial for the value of this parameter.

The methyl torsional barrier of  $34.1\text{ cm}^{-1}$  in 2MTA is much lower than that found in the oxygen analog 2-methyloxazole ( $252\text{ cm}^{-1}$ ).<sup>18,30</sup> This is in agreement with the trend observed for the monomethyl derivatives of furan and thiophene, e.g., 2-methylfuran ( $416.2\text{ cm}^{-1}$ )<sup>31</sup> vs 2-methylthiophene ( $194.1\text{ cm}^{-1}$ )<sup>29</sup> and 3-methylfuran ( $380.5\text{ cm}^{-1}$ )<sup>32</sup> vs 3-methylthiophene ( $258.8\text{ cm}^{-1}$ ).<sup>33</sup> The same is also found for the dimethyl substituted versions with the only example 2,5-dimethylfuran ( $439.2\text{ cm}^{-1}$ )<sup>34</sup> vs 2,5-dimethylthiophene ( $248.0\text{ cm}^{-1}$ ).<sup>35</sup>

## V. CONCLUSION

The microwave spectrum of 2MTA containing a methyl group attached on the second position of the thiazole ring was assigned under molecular jet conditions with supports from quantum chemistry. Highly accurate molecular parameters were determined using the programs *XIAM* and *BELGI-C<sub>s</sub>-hyperfine*. The internal rotation of the methyl group causes torsional splittings of all rotational transitions into the A and E species, which are additionally complicated by the quadrupole coupling arising from the <sup>14</sup>N nucleus. Using the *XIAM* code, the whole dataset was reproduced with a root-mean-square deviation of 455.9 kHz, while the *BELGI-C<sub>s</sub>-hyperfine* code reduced this value to 3.2 kHz. The barrier to internal rotation of about  $34\text{ cm}^{-1}$  is the lowest observed in three isomers of methylthiazole. Comparison to other methyl substituted sulfur-containing five-membered rings leads to the conclusion that not only the position of the methyl group but also the presence of the nitrogen atom strongly influences the barrier height. The results found for 2MTA also confirm the trend that the ring methyl torsion has a lower barrier in the sulfur analog than that in the oxygen analog.

## SUPPLEMENTARY MATERIAL

See the [supplementary material](#) for the Cartesian coordinates, data points of the potential energy curves, and the frequency list. The *XIAM* and *BELGI-C<sub>s</sub>-hyperfine* inputs and outputs are available as separate files. The *BELGI-C<sub>s</sub>-hyperfine* code is currently available with one of the authors (I.K.).

## ACKNOWLEDGMENTS

T.N. thanks the Department of Space and Aeronautics, University of Science and Technology of Hanoi, Vietnam, for a USTH scholarship for excellent students Bachelor program, the Faculty of Sciences and Technology of University Paris-Est Créteil for a fellowship during her Master thesis, and the University of Paris for a Ph.D. Grant. V.V. is grateful to the Fonds der Chemischen Industrie for a Ph.D. fellowship. W.S. thanks the University Paris Est for an invited researcher grant, which enabled him to work at LISA. Alina Wildenberg and Ba Thanh Dang are acknowledged for performing some of the measurements during their student research projects. We thank Dr. Yannick Giraud-Héraud and Professor Ngo Duc Thanh for their help and support in the master thesis of T.N. at LISA and Professor Stefan Willitsch for helpful discussions on the zero-point energy. This work was supported by the Agence

Nationale de la Recherche ANR (Project ID ANR-18-CE29-0011) and the Programme National “Physique et Chimie du Milieu Interstellaire” (PCMI) of CNRS/INSU with INC/INP co-funded by CEA and CNES.

## REFERENCES

- 1 R. C. Woods, *J. Mol. Spectrosc.* **22**, 49 (1967).
- 2 H. Hartwig and H. Dreizler, *Z. Naturforsch. A* **51**, 923 (1996).
- 3 J. T. Hougen, I. Kleiner, and M. Godefroid, *J. Mol. Spectrosc.* **163**, 559 (1994).
- 4 I. Kleiner and J. T. Hougen, *J. Chem. Phys.* **119**, 5505 (2003).
- 5 P. Groner, *J. Chem. Phys.* **107**, 4483 (1997).
- 6 V. V. Ilyushin, Z. Kisiel, L. Pszczółkowski, H. Mäder, and J. T. Hougen, *J. Mol. Spectrosc.* **259**, 26 (2010).
- 7 D. F. Plusquellic, R. D. Suenram, B. Maté, J. O. Jensen, and A. C. Samuels, *J. Chem. Phys.* **115**, 3057 (2001).
- 8 See <http://spec.jpl.nasa.gov/> for downloading and instruction of the program.
- 9 I. Kleiner, *ACS Earth Space Chem.* **3**, 1812 (2019).
- 10 A. Belloche, A. A. Meshcheryakov, R. T. Garrod, V. V. Ilyushin, E. A. Alekseev, R. A. Motiyenko, L. Margulès, H. S. P. Müller, and K. M. Menten, *Astron. Astrophys.* **601**, A49 (2017).
- 11 R. Kannengießler, W. Stahl, H. V. L. Nguyen, and I. Kleiner, *J. Phys. Chem. A* **120**, 3992 (2016).
- 12 A. Roucou, I. Kleiner, M. Goubet, S. Bteich, G. Mouret, R. Bocquet, F. Hindle, W. L. Meerts, and A. Cuisset, *ChemPhysChem* **19**, 1056 (2018).
- 13 T. Nguyen, C. Dindic, W. Stahl, H. V. L. Nguyen, and I. Kleiner, *Mol. Phys.* **1668572** (2019).
- 14 J.-U. Grabow, H. Hartwig, N. Heineking, W. Jäger, H. Mäder, H. W. Nicolaisen, and W. Stahl, *J. Mol. Struct.* **612**, 349 (2002).
- 15 H.-W. Nicolaisen, J.-U. Grabow, N. Heineking, and W. Stahl, *Z. Naturforsch. A* **46**, 635 (1991).
- 16 W. Jäger and H. Mäder, *Z. Naturforsch. A* **42**, 1405 (1987).
- 17 W. Jäger and H. Mäder, *J. Mol. Struct.* **190**, 295 (1988).
- 18 E. Fliege, H. Dreizler, M. Meyer, K. Iqbal, and J. Sheridan, *Z. Naturforsch. A* **41**, 623 (1986).
- 19 M. J. Frisch, G. W. Trucks, H. B. Schlegel, G. E. Scuseria, M. A. Robb, J. R. Cheeseman, J. A. Montgomery, Jr., T. Vreven, K. N. Kudin, J. C. Burant, J. M. Millam, S. S. Iyengar, J. Tomasi, V. Barone, B. Mennucci, M. Cossi, G. Scalmani, N. Rega, G. A. Petersson, H. Nakatsuji, M. Hada, M. Ehara, K. Toyota, R. Fukuda, J. Hasegawa, M. Ishida, T. Nakajima, Y. Honda, O. Kitao, H. Nakai, M. Klene, X. Li, J. E. Knox, H. P. Hratchian, J. B. Cross, V. Bakken, C. Adamo, J. Jaramillo, R. Gomperts, R. E. Stratmann, O. Yazyev, A. J. Austin, R. Cammi, C. Pomelli, J. W. Ochterski, P. Y. Ayala, K. Morokuma, G. A. Voth, P. Salvador, J. J. Dannenberg, V. G. Zakrzewski, S. Dapprich, A. D. Daniels, M. C. Strain, O. Farkas, D. K. Malick, A. D. Rabuck, K. Raghavachari, J. B. Foresman, J. V. Ortiz, Q. Cui, A. G. Baboul, S. Clifford, J. Cioslowski, B. B. Stefanov, G. Liu, A. Liashenko, P. Piskorz, I. Komaromi, R. L. Martin, D. J. Fox, T. Keith, M. A. Al-Laham, C. Y. Peng, A. Nanayakkara, M. Challacombe, P. M. W. Gill, B. Johnson, W. Chen, M. W. Wong, C. Gonzalez, and J. A. Pople, *Gaussian03, Revision D.01*, Gaussian, Inc., Wallingford, CT, 2004.
- 20 H. B. Schlegel, *J. Comput. Chem.* **3**, 214–218 (1982).
- 21 J. U. Grabow, W. Stahl, and H. Dreizler, *Rev. Sci. Instrum.* **67**, 4072 (1996).
- 22 I. Merke, W. Stahl, and H. Dreizler, *Z. Naturforsch. A* **49**, 490 (1994).
- 23 D. Jelisavac, D. C. Cortés Gómez, H. V. L. Nguyen, L. W. Sutikdja, W. Stahl, and I. Kleiner, *J. Mol. Spectrosc.* **257**, 111 (2009).
- 24 W. C. Bailey, Calculation of nuclear quadrupole coupling constants in gaseous state molecules, <http://nqcc.wcbailey.net/index.html>.
- 25 R. Kannengießler, S. Klahm, H. V. L. Nguyen, A. Lüchow, and W. Stahl, *J. Chem. Phys.* **141**, 204308 (2014).
- 26 M. Andresen, I. Kleiner, M. Schwell, W. Stahl, and H. V. L. Nguyen, *J. Phys. Chem. A* **124**, 1353 (2020).
- 27 A. Jabri, V. Van, H. V. L. Nguyen, W. Stahl, and I. Kleiner, *ChemPhysChem* **17**, 2660 (2016).

<sup>28</sup>V. Van, W. Stahl, and H. V. L. Nguyen, *ChemPhysChem* **17**, 3223 (2016).

<sup>29</sup>N. M. Pozdeev, L. N. Gunderova, and A. A. Shapkin, *Opt. Spektrosk.* **28**, 254 (1970).

<sup>30</sup>E. R. L. Fliege, *Z. Naturforsch. A* **45**, 911 (1990).

<sup>31</sup>I. A. Finneran, S. T. Shipman, and S. L. Widicus Weaver, *J. Mol. Spectrosc.* **280**, 27 (2012).

<sup>32</sup>T. Ogata and K. Kozima, *Bull. Chem. Soc. Jpn.* **44**, 2344 (1971).

<sup>33</sup>T. Ogata and K. Kozima, *J. Mol. Spectrosc.* **42**, 38 (1972).

<sup>34</sup>V. Van, J. Bruckhuisen, W. Stahl, V. Ilyushin, and H. V. L. Nguyen, *J. Mol. Spectrosc.* **343**, 121 (2018).

<sup>35</sup>V. Van, W. Stahl, and H. V. L. Nguyen, *Phys. Chem. Chem. Phys.* **17**, 32111 (2015).